

**Systematic investigation of REE mobility and fractionation during
continental shale weathering along a climate gradient**

Principal investigators:

Lin Ma and Lixin Jin

Department of Geological Sciences, University of Texas at El Paso, 500 W. University Ave., El Paso, TX 79968

Project collaborators:

Ashlee Dere, Timothy White, and Susan Brantley

Earth and Environmental Systems Institute, Pennsylvania State University, University Park, PA 16802

Research supported by the U.S. Geological Survey (USGS), Department of the Interior, under USGS award number G12AP20050. The views and conclusions contained in this document are those of the authors and should not be interpreted as necessarily representing the official policies, either expressed or implied, of the U.S. Government.

1. Introduction

Rare earth elements (REE) have been identified as crucial and strategic natural resources. The demand for REE in the United States is increasing rapidly, especially as industrial compounds for novel electronic and green-energy products (e.g., USGS, 2011). REEs are relatively abundant in the Earth's crust, but REE deposits with minable concentrations are uncommon. One recent study by Kato et al (2010) has pointed to the deep-sea REE-rich muds in the Pacific Ocean as a new potential resource. The formation of these muds is related to adsorption and concentration of REE from seawater by hydrothermal iron-oxyhydroxides and phillipsite (Kato et al., 2010). Understanding global REE cycles at Earth's surface, such as mobility of REEs through chemical weathering and their transport and deposition, will facilitate finding new REE deposits. At present, the mechanisms and factors controlling release, transport, and deposition of REE - the sources and sinks - at Earth's surface remain unclear.

Weathering of continental rocks is important in global elemental cycles including REEs. During the transformation of bedrock into soils, REEs are leached into natural waters and transported to oceans. The REE hosted in easily weathered minerals become depleted from soil profiles at early stages of rock alteration, while those in relatively stable mineral phases remain in the solid soils for longer duration. The retention of dissolved REEs on soils and suspended particles in water, however, also depends on their affinity to secondary phases, especially Fe/Al oxyhydroxides and phosphate phases. In shales, especially organic-rich black shales, REE and other trace metals are largely associated with phosphates, carbonate, and clay minerals (e.g., Lev and Filer, 2004). The presence of organic matter, carbonates and sulfides in shales greatly enhances the release of REEs and other metals to surface environments during shale weathering. For example, our previous REE study has shown that significant amounts of REEs are released and mobilized during gray shale weathering in central Pennsylvania (Ma et al., 2011).

The formation of soils has long been considered as a function of climate, topography, organisms, type of parent material, and soil age (Jenny, 1941). A gradient approach has often been used to understand the influence of each variable (e.g. Bockheim, 1980; Birkeland, 1999; Williams et al., 2010), including chronosequences (age) and climosequences (climate). Here, we systematically studied soil profiles and bedrock in seven watersheds that are developed on gray shale bedrock along a climate transect in the eastern USA and Wales (Fig. 1) to constrain the mobility and fractionation of REE during early stages of chemical weathering. In addition, one site on black shale bedrock in Pennsylvania was included to allow comparison of behaviors of REEs in the organic-rich vs. organic-poor shale end members under the same environmental conditions. Our main objectives are to investigate: 1) the abundance of REEs in both gray and black shales and the dissolution kinetics of these REE-bearing minerals along the climate gradient 2) the biogeochemical and hydrological conditions (such as cation exchange capacity, dissolved organic carbon and pH) that dictate the mobility and fractionation of REEs in surface and subsurface

environments (Patino et al., 2003; Ma et al., 2011), and 3) the retention of REEs in soils under different redox conditions. This systematic study sheds light on the geochemical behaviors and environmental pathways of REEs during continental shale weathering.

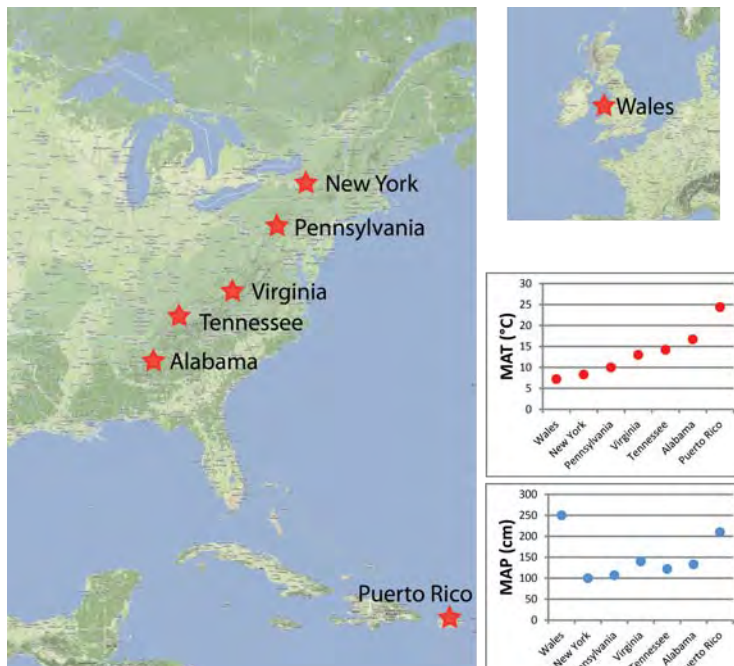


Figure 1. Location and climate information for shale transect sites used in this study (after Dere et al., 2013). MAP=mean annual precipitation; MAT=mean annual temperature.

2. Geological setting

2.1. Sites description

In this study, we used five field sites that were carefully selected by a previous study (Dere et al., 2013) along a climate gradient primarily on the same shale unit within the Appalachian Mountains (New York (NY), Pennsylvania (PA), Virginia (VA), Tennessee (TN), and Alabama (AL)), holding other variables as constant as possible (Figure 1; Table 1). Two more field sites include a tropical site in Puerto Rico (PR) and a cold/wet site in Wales, United Kingdom. We intentionally focused on the same parent material bedrock composition by choosing sites that are located on Silurian gray shale, known as the Rose Hill Formation of the Clinton Group in NY, PA, and VA, the Rockwood Formation in TN, the Red Mountain Formation in AL, and the Gwestyn Formation in Wales. In PR, the Oligocene San Sebastian Formation was identified as the most stratigraphically and geochemically similar formation in PR to the Rose Hill Formation. In addition, a site on Devonian black shale (Marcellus Formation) was selected in

Huntington, PA and this site allows comparison of behaviors of REEs in the organic-rich and organic-poor shale end-members under the same environmental conditions in Pennsylvania.

Table 1. Shale weathering transect site characteristics (after Dere et al., 2013)

Site	Latitude	Longitude	Elevation (m)	MAT (°C)	MAP (cm)	Soil thickness (cm)	Soil residence time (ka)
Wale, UK	N52° 28.416	W3° 41.575	417	7.2	250	35	10
New York (NY)	N43° 1.739	W75° 16.609	269	8.3	106	220	10
Pennsylvania (PA)	N40° 39.931	W77° 54.297	297	10	107	28	17
Virginia (VA)	N37° 55.625	W79° 32.799	752	11	106	80	47
Tennessee (TN)	N36° 16.414	W83° 54.809	418	14	138	398	234
Alabama (AL)	N34° 25.375	W86° 12.400	241	16	136	220	129
Puerto Rico (PR)	N18° 18.050	W66° 54.401	366	24	234	613	253

MAT=mean annual temperature, and MAP=mean annual precipitation.

2.2 Climate gradient

Mean annual temperature (MAT) and mean annual precipitation (MAP) were estimated for each site using data from proximal weather stations at similar elevations with at least 20 yr of complete records (Dere et al., 2013; Table 1). Along the east coast of United States, the climate is characterized by a cold and dry end-member in New York and a warm and wet end-member in Puerto Rico (Figure 1). Wales is an outlier, with low MAT but high MAP. Moreover, as discussed below, NY site was developed on glacial till, different from other sites.

2.3 Soil residence time

Soil residence time (SRT) is defined as the average time that a particle resides in a soil, after a soil is formed from a parent but before being eroded away. Thus SRT is a good estimate how long minerals in soil particles have been weathered. SRT of all soil profiles, reported by Dere et al. (2013) and discussed in Dere (2014), are summarized in Table 1 and introduced briefly below. The maximum SRT estimated is for the PR site (250 ka) where the largest climate transition occurred from marine isotope stage (MIS) 5 to the Last Glacial Maximum (LGM) (~ 5°C) (Imbrie et al., 1984). The other soils have an estimated SRT less than 100 ka. Over that time period, the largest climate change in North America

occurred during the transition from LGM to the present (Cadwell et al., 2004; Clark et al., 2004). The LGM directly impacted Wales and NY by glaciation, while PA was subjected to periglacial conditions until at least 15 ka (Ciolkosz et al., 1986; Clark and Ciolkosz, 1988; Gardner et al., 1991). Previous researchers have also found periglacial features present in VA and the Great Smoky Mountains in TN (King and Ferguson, 1960; Clark and Ciolkosz, 1988). For all our sites in this study, residual shale soil was developed on bedrock except for the NY where a parent material that consisted of locally-derived shale till.

3. Methods

3.1. Rock and soil sampling

The rock and soil samples were previously collected and characterized for major chemistry, mineralogy, and soil properties including soil pH and bulk density (Dere et al., 2013). Sampling method is provided briefly below.

Only ridge-top soils were selected for investigation to avoid the complexity of downslope sediment transport and thus changes in soil chemistry and mineralogy were entirely due to in-situ shale weathering (Jin et al., 2010). Soils used here are operationally as the material that can be augered or dug by hand. Saprock, the layer between a soil and underlying bedrock, was chemically altered and different from bedrock, but retain the bedrock layout and can not be augered (below layer of refusal). At the grey shale site in PA, Jin et al. (2011) argued that fresh bedrock was only encountered at depths of 26 m at ridges and that an intervening layer of “saprock” was found between fresh bedrock and soil. The weathering profiles in Wales and PA are comprised of a soil overlying rock without intervening saprolite. Soils in NY are developed from glacial till. In VA, soil is developed from shale that extends right into the weathered sandstone layer below (~80cm deep). Weathering profiles in TN, AL, and PR consist of soils overlying saprolite. Field augering did not penetrate into saprock or fresh bedrock beneath the soils at TN, AL, and PR.

Soil samples were collected using a 5-cm diameter hand auger from the mineral soil surface to the depth of refusal, where auger penetration is impossible. Soils were sampled at 5-cm interval in the upper 20 cm of the soil and then at 10-cm interval below that. The organic horizon was collected separately by hand before augering and the interface between the organic and mineral horizon was defined as depth 0 cm. In addition to hand augering, soil pits were hand dug as deeply as possible (maximum depth of 2 m) and described (Soil Survey Staff, 1993).

To constrain parent composition, bedrock samples were collected both from outcrops nearby and from soil pits as chips. A drill core (DC-1) at the PA site (Shale Hills catchment) was used and deep portions are characterized as the gray shale parent bedrock. At the black shale site in PA, rock chips from

Table 2. REE and Zr concentrations (in ppm) of parent materials including shale chips and deepest soils from the soil profile and local outcrops.

Site	Sample		La	Ce	Pr	Nd	Sm	Eu	Gd	Tb	Dy	Ho	Er	Tm	Yb	Lu	Zr	
	Name	Type																
Wales	Q31-35	deepest soil	54.0	132.0	13.3	47.3	8.3	1.9	6.5	1.0	5.6	1.2	3.4	0.5	3.3	0.5	166.0	
	Q-RF	shale chip	21.3	55.3	5.9	22.5	4.9	1.2	5.1	0.8	5.4	1.1	3.5	0.5	3.3	0.5	164.0	
	ALD-10-01	local outcrop	34.5	73.5	7.7	25.8	5.4	1.4	5.2	0.9	5.5	1.2	3.2	0.5	3.1	0.5	157.0	
	ALD-10-02	local outcrop	212.0	454.0	53.8	177.0	29.4	5.8	15.0	1.7	8.2	1.4	3.7	0.5	3.4	0.5	164.0	
	ALD-10-03	local outcrop	17.6	43.9	5.1	18.4	3.9	1.0	3.6	0.6	4.2	0.9	2.6	0.4	2.8	0.4	164.0	
	ALD-10-04	local outcrop	69.5	163.0	19.4	65.9	12.1	2.5	7.5	1.0	5.9	1.2	3.3	0.5	3.3	0.5	219.0	
	ALD-10-06	local outcrop	55.6	103.0	10.8	33.8	6.0	1.4	5.0	0.9	5.4	1.1	3.2	0.5	3.3	0.5	190.0	
	ALD-10-07	local outcrop	19.2	42.3	4.7	17.1	4.3	1.1	4.6	0.8	5.4	1.2	3.4	0.5	3.5	0.5	207.0	
	ALD-10-08	local outcrop	17.9	35.9	3.9	13.3	3.1	0.9	4.1	0.8	5.1	1.1	3.2	0.5	3.2	0.5	180.0	
	ALD-10-09	local outcrop	19.5	44.9	5.5	20.3	4.8	1.2	4.7	0.8	4.9	1.1	2.9	0.5	3.0	0.5	169.0	
	ALD-10-33	local outcrop	39.3	86.7	9.8	33.9	6.8	1.6	5.3	0.8	5.1	1.1	2.9	0.5	3.1	0.5	137.0	
		<i>Ave</i>		50.6	110.3	12.7	42.8	8.1	1.8	6.0	0.9	5.5	1.1	3.2	0.5	3.2	0.5	175.1
		<i>Stdev</i>		59.4	126.8	15.2	49.5	7.9	1.5	3.3	0.3	1.0	0.1	0.3	0.0	0.2	0.0	24.4
PA	SPRT 2030	deepest soil/gray shale	36.9	70.8	9.5	31.2	6.1	1.1	4.7	0.9	4.6	1.0	2.9	0.4	2.9	0.4	246.0	
	Average DC-1	local bedrock/gray shale	50.5	98.9	13.2	46.1	9.0	1.7	7.3	1.2	6.3	1.4	3.8	0.5	3.8	0.6	178.0	
	AF-1-15	deepest soil/black shale	47	106	11.4	43.8	8.7	1.67	7.56	1.12	6.51	1.28	3.62	0.5	3.6	0.55	146.0	
	AF-1-17	local bedrock/black shale	68.7	241	17.8	72.1	15.7	3.39	15.3	2.33	13	2.57	7.01	1.05	6.9	1.08	159.0	
NY	ALD-10-40	deepest soil	17.9	41.5	4.9	19.0	4.4	0.9	3.9	0.6	3.5	0.7	2.0	0.3	1.9	0.3	299.0	
VA	MT-09-39	deepest soil	69.4	126.0	15.1	58.7	11.7	2.6	14.8	2.4	15.0	3.3	9.3	1.3	7.7	1.1	882.0	
	TSW-1163	local outcrop	52.6	108.0	13.3	45.2	8.6	1.6	6.5	1.1	7.3	1.6	4.7	0.8	4.9	0.8	311.0	
	TSW-1164	local outcrop	53.5	116.0	14.0	48.3	8.9	1.7	6.5	1.1	7.1	1.6	4.5	0.7	4.8	0.7	338.0	
	TSW-1165	local outcrop	48.5	98.4	12.2	42.1	8.7	1.8	7.2	1.2	7.5	1.6	4.7	0.8	4.8	0.7	217.0	
		<i>Ave</i>		51.5	107.5	13.2	45.2	8.7	1.7	6.7	1.1	7.3	1.6	4.6	0.7	4.8	0.7	288.7
		<i>Stdev</i>		2.7	8.8	0.9	3.1	0.2	0.1	0.4	0.1	0.2	0.0	0.1	0.0	0.1	0.0	63.5
TN	ALD-11-432	deepest soil	53.1	112.0	13.6	49.3	9.2	1.7	8.2	1.3	7.9	1.6	4.7	0.7	4.4	0.7	268.0	
	ALD-10-432	shale chip	51.6	103.0	12.4	48.2	8.6	1.7	8.3	1.2	7.3	1.6	4.6	0.7	4.4	0.7	261.0	
	TSW-1212	local outcrop	56.2	114.0	14.6	50.8	10.0	1.9	8.0	1.3	7.9	1.7	4.7	0.7	4.7	0.7	256.0	
	TSW-1213	local outcrop	53.2	105.0	13.3	45.1	8.6	1.6	6.8	1.1	7.1	1.5	4.5	0.7	4.5	0.7	247.0	
	TSW-1214	local outcrop	54.6	112.0	14.2	49.0	9.5	1.9	7.6	1.2	7.7	1.6	4.5	0.7	4.6	0.7	272.0	
		<i>Ave</i>		53.9	108.5	13.6	48.3	9.2	1.8	7.7	1.2	7.5	1.6	4.6	0.7	4.6	0.7	259.0
	<i>Stdev</i>		2.0	5.3	1.0	2.4	0.7	0.1	0.7	0.1	0.4	0.1	0.1	0.0	0.1	0.0	10.4	
AL	ALD-11-508	deepest soil	75.9	99.0	17.9	86.9	21.4	4.6	17.6	1.7	6.9	1.0	2.5	0.3	2.2	0.4	148.0	
	ALD-10-2025	local outcrop	57.8	110.0	15.6	54.6	12.1	2.5	11.1	1.8	10.1	2.1	5.5	0.8	5.2	0.8	165.0	
	ALD-10-2026	local outcrop	60.1	123.0	17.3	63.5	14.8	3.1	13.9	2.1	12.3	2.5	6.5	1.0	5.8	0.9	219.0	
	ALD-10-2028	local outcrop	50.7	99.5	13.1	45.3	9.1	1.8	7.5	1.2	7.3	1.6	4.4	0.7	4.3	0.6	226.0	
		<i>Ave</i>		56.2	110.8	15.3	54.5	12.0	2.4	10.8	1.7	9.9	2.1	5.5	0.8	5.1	0.8	203.3
		<i>Stdev</i>		4.9	11.8	2.1	9.1	2.9	0.6	3.2	0.5	2.5	0.5	1.1	0.2	0.8	0.1	33.4
PR	ALD-11-92	deepest soil	50.6	61.4	12.2	54.9	11.8	3.7	13.3	1.9	11.1	2.2	6.4	0.9	5.6	0.9	114.0	
	ALD-11-93	local outcrop	9.8	22.5	3.1	14.5	2.8	0.8	2.9	0.4	2.3	0.5	1.5	0.2	1.4	0.2	49.4	
	ALD-11-03	local outcrop	37.2	25.6	5.0	21.9	3.7	1.1	4.9	0.6	3.4	0.7	2.0	0.3	1.5	0.2	54.7	
		<i>Ave</i>		23.5	24.1	4.1	18.2	3.3	0.9	3.9	0.5	2.9	0.6	1.7	0.2	1.5	0.2	52.1
		<i>Stdev</i>		19.4	2.2	1.3	5.2	0.6	0.2	1.4	0.1	0.7	0.2	0.4	0.0	0.1	0.0	3.7

Table 3. Ranges of REE concentrations (in ppm) in all eight soil profiles.

Site	Total Depth (cm)		La	Ce	Pr	Nd	Sm	Eu	Gd	Tb	Dy	Ho	Er	Tm	Yb	Lu	Total REE
Wales	35	N=5															
		Min	39.0	90.9	9.6	31.2	5.5	1.27	4.52	0.73	4.39	0.88	2.51	0.37	2.60	0.38	200.0
		Max	54.0	132	13.3	47.3	8.3	1.87	6.45	1.02	5.61	1.16	3.37	0.50	3.30	0.46	278.6
		Median	42.6	94.2	9.8	34.0	6.7	1.42	5.56	0.89	4.93	1.01	2.96	0.46	3.00	0.45	207.1
		Stdev	5.9	17.0	1.6	6.5	1.0	0.24	0.76	0.11	0.51	0.11	0.36	0.05	0.26	0.03	33.0
PA (gray shale)	25	N=3															
		Min	36.9	70.8	9.0	31.0	5.7	1.10	4.71	0.85	4.63	1.02	2.92	0.39	2.90	0.43	173.4
		Max	42.4	82.8	10.6	36.0	6.8	1.20	5.47	0.98	5.34	1.13	3.34	0.45	3.30	0.52	200.3
		Median	37.6	72.0	9.5	31.2	6.1	1.10	4.75	0.86	4.74	1.03	2.97	0.39	3.10	0.43	174.7
		Stdev	3.0	6.6	0.8	2.8	0.6	0.06	0.43	0.07	0.38	0.06	0.23	0.03	0.20	0.05	15.2
PA (Black shale)	171	N=8															
		Min	24.9	53.2	5.9	22.4	4.2	0.82	3.76	0.57	3.42	0.69	2.03	0.29	2.00	0.29	124.5
		Max	58.0	139	15.9	67.3	16.2	3.50	15.0	2.08	11.0	2.05	5.48	0.77	5.20	0.77	342.3
		Median	45.7	100	10.9	40.6	7.2	1.38	6.23	0.98	5.68	1.21	3.55	0.50	3.55	0.55	230.3
		Stdev	9.4	24.4	2.8	13.0	3.7	0.86	3.56	0.46	2.32	0.40	1.01	0.14	0.93	0.14	61.7
New York	230	N=14															
		Min	17.9	41.5	4.9	19.0	4.0	0.79	3.30	0.59	3.54	0.71	1.97	0.30	1.90	0.27	101.9
		Max	29.0	79.7	8.8	35.4	9.2	1.96	8.88	1.24	7.08	1.31	3.64	0.52	3.20	0.45	169.0
		Median	24.2	58.0	6.6	24.3	5.0	1.05	4.32	0.70	4.24	0.86	2.45	0.37	2.50	0.36	134.0
		Stdev	3.4	11.7	1.0	4.0	1.3	0.30	1.43	0.17	0.93	0.15	0.38	0.05	0.29	0.04	19.9
VA	80	N=8															
		Min	39.8	85.4	9.6	38.5	6.9	1.40	6.60	0.92	5.61	1.22	3.53	0.52	3.40	0.55	204.5
		Max	69.4	126	16.8	65.9	19.4	6.54	47.1	9.25	51.7	10.6	27.8	3.93	19.2	3.15	469.7
		Median	49.8	105	11.7	45.4	8.4	1.76	8.70	1.29	8.00	1.75	5.10	0.72	4.80	0.74	252.5
		Stdev	10.9	15.4	2.6	10.0	4.1	1.72	13.6	2.83	15.5	3.17	8.13	1.15	5.25	0.87	87.8
TN	398	N=22															
		Min	39.5	84.1	9.8	33.2	5.9	1.12	5.27	0.90	5.83	1.19	3.33	0.51	3.50	0.49	194.8
		Max	63.9	131	16.3	61.2	13.1	2.45	9.79	1.43	8.01	1.62	4.67	0.70	4.50	0.67	304.4
		Median	52.4	110	13.1	45.7	8.2	1.46	6.35	1.04	6.24	1.27	3.74	0.55	3.70	0.54	257.1
		Stdev	6.1	12.3	1.7	6.4	1.5	0.28	1.11	0.14	0.63	0.12	0.33	0.05	0.27	0.05	29.0
AL	200	N=12															
		Min	17.5	30.8	3.7	14.7	2.6	0.54	2.62	0.37	2.39	0.54	1.58	0.22	1.50	0.23	79.4
		Max	123	163	34.2	187	47.0	10.2	37.7	3.68	13.5	1.80	3.93	0.45	2.70	0.42	627.8
		Median	55.1	70.8	12.6	57.0	13.2	2.87	11.0	1.13	4.65	0.79	2.31	0.31	2.25	0.35	227.8
		Stdev	36.4	45.1	11.2	61.9	15.9	3.49	2	1.17	3.81	0.42	0.72	0.07	0.38	0.06	191.7
PR	632	N=18															
		Min	4.1	8.9	0.9	3.7	0.8	0.25	1.07	0.19	1.34	0.34	1.09	0.18	1.20	0.19	25.2
		Max	73.2	108	17.8	79.6	17.0	5.30	18.1	2.54	14.5	2.88	7.98	1.10	6.50	0.97	355.5
		Median	7.0	26.2	1.9	8.2	1.8	0.52	1.87	0.31	1.91	0.44	1.48	0.23	1.75	0.28	54.0
		Stdev	18.5	24.9	4.5	20.2	4.3	1.34	4.61	0.63	3.59	0.70	1.88	0.25	1.44	0.21	86.1

Table 4 Cation exchange capacity in soil profiles

Site	Depth cm										(Ca+Mg)/ Al	
		Al mmol/ Kg	Ca mmol/ Kg	Fe mmol/ Kg	K mmol/ Kg	Mg mmol/ Kg	Mn mmol/ Kg	Na mmol/ Kg	Si mmol/ Kg	Sr mmol/ Kg	CEC cmolc/kg	Al
Wales	0	14.44	0.29	1.77	1.12	1.24	0.53	1.09	0.05	0.00	5.52	0.11
	10	9.34	0.24	0.08	0.74	0.53	5.97	0.76	0.04	0.01	4.34	0.08
	20	3.90	0.09	0.03	0.30	0.23	1.57	0.33	0.02	0.01	1.63	0.08
	31	1.96	0.06	0.03	0.23	0.18	0.39	0.20	0.04	0.01	0.78	0.12
VA	0	4.13	4.56	0.01	1.75	1.06	10.74	0.05	0.06	0.03	4.72	1.36
	10	4.33	1.29	0.01	0.58	0.46	5.04	0.01	0.06	0.02	2.74	0.40
	20	7.56	0.81	0.01	0.41	0.30	2.62	0.00	0.08	0.01	3.09	0.15
	30	19.49	1.28	0.02	0.69	0.95	1.22	0.02	0.15	0.02	6.67	0.11
	40	24.70	1.49	0.02	0.85	2.16	1.20	0.01	0.17	0.02	8.54	0.15
	50	24.07	0.83	0.02	0.94	2.77	0.60	0.03	0.16	0.02	8.23	0.15
	60	15.45	0.28	0.02	0.63	1.99	0.33	0.00	0.09	0.01	5.26	0.15
TN	70	12.62	0.21	0.02	0.58	1.67	0.56	0.00	0.07	0.01	4.37	0.15
	0	25.52	2.82	0.78	2.00	1.47	1.10	0.00	0.04	0.02	9.19	0.17
	5	22.37	0.57	0.14	1.69	0.71	0.80	0.00	0.06	0.00	7.36	0.06
	10	18.55	0.84	0.02	1.99	0.99	1.14	0.00	0.13	0.01	6.41	0.10
	20	17.57	0.72	0.01	2.70	1.20	2.39	0.00	0.16	0.01	6.47	0.11
	30	18.89	0.46	0.01	2.35	1.55	0.73	0.00	0.16	0.01	6.52	0.11
	40	22.14	0.68	0.03	2.30	2.44	0.10	0.00	0.16	0.01	7.59	0.14
	50	27.93	0.42	0.03	2.58	3.43	0.05	0.00	0.18	0.01	9.50	0.14
	70	26.70	0.17	0.02	2.40	3.06	0.03	0.00	0.25	0.00	9.01	0.12
	90	24.48	0.08	0.02	2.25	2.92	0.02	0.03	0.31	0.00	8.31	0.12
	110	19.79	0.06	0.01	1.70	2.68	0.03	0.04	0.29	0.00	6.79	0.14
	130	28.00	0.07	0.02	2.36	4.22	0.05	0.17	0.21	0.00	9.61	0.15
	150	26.15	0.07	0.02	2.48	4.40	0.08	0.20	0.24	0.01	9.13	0.17
	155	25.31	0.08	0.02	2.50	4.30	0.04	0.19	0.26	0.00	8.85	0.17
	170	24.63	0.14	0.02	2.56	5.47	0.07	0.32	0.32	0.00	8.95	0.23
	200	22.06	0.12	0.03	2.71	5.92	0.10	0.41	0.20	0.00	8.25	0.27
	220	20.90	0.08	0.01	2.68	6.77	0.16	0.47	0.32	0.01	8.12	0.33
	240	20.55	0.10	0.01	2.70	7.40	0.44	0.49	0.33	0.00	8.21	0.37
	250	16.53	0.27	0.02	3.45	9.10	0.15	0.76	0.36	0.01	7.43	0.57
	290	14.07	0.24	0.01	3.12	9.62	0.23	0.63	0.31	0.00	6.74	0.70
330	14.04	0.30	0.01	3.36	12.17	0.49	0.72	0.32	0.01	7.34	0.89	
360	10.72	0.22	0.02	3.90	13.55	0.60	0.68	0.28	0.01	6.66	1.28	
388	9.48	0.47	0.01	4.57	15.46	0.81	0.72	0.33	0.01	6.86	1.68	
AL	0	4.49	1.51	0.03	1.21	0.48	0.90	0.00	0.02	0.01	2.07	0.44
	10	3.89	0.71	0.02	0.89	0.40	0.85	0.00	0.04	0.01	1.67	0.28
	20	6.27	0.80	0.01	0.97	0.37	0.83	0.00	0.09	0.01	2.42	0.19
	30	13.19	1.26	0.05	1.89	0.92	0.81	0.00	0.14	0.02	4.81	0.17
	40	13.89	1.39	0.03	2.08	3.27	0.70	0.00	0.22	0.02	5.54	0.34
	70	25.27	0.55	0.02	1.57	6.70	0.19	0.00	0.51	0.01	9.44	0.29
	90	27.80	0.38	0.01	1.15	4.68	0.19	0.00	0.73	0.01	9.80	0.18
	100	29.00	0.26	0.02	1.19	3.74	0.11	0.04	0.67	0.01	9.92	0.14
	120	33.01	0.25	0.01	1.20	3.32	0.13	0.01	0.76	0.01	11.07	0.11
	140	22.33	0.70	0.02	0.97	2.16	0.33	0.02	0.49	0.02	7.64	0.13
	155	26.92	0.14	0.03	0.83	1.71	0.03	0.00	0.54	0.01	8.76	0.07
	180	26.13	0.58	0.03	0.92	2.35	0.08	0.00	0.66	0.01	8.81	0.11
	200	25.61	0.68	0.02	0.94	2.35	0.32	0.04	0.49	0.01	8.66	0.12
	PR	0	0.00	132.98	0.01	7.91	16.36	0.15	1.59	0.59	0.22	31.11
8		0.00	117.53	0.02	4.60	13.40	0.13	1.91	0.54	0.20	27.11	13092
10		0.00	109.94	0.02	3.02	11.64	0.12	2.18	0.51	0.18	25.09	12158
15		0.00	98.92	0.01	2.39	10.22	0.08	2.86	0.47	0.18	22.58	10913
20		0.00	89.35	0.02	2.51	8.62	0.02	2.84	0.40	0.17	20.31	9797
30		0.00	83.89	0.02	2.66	7.27	0.01	2.44	0.32	0.15	18.89	9116
40		0.00	77.45	0.02	3.12	7.14	0.00	2.23	0.32	0.14	17.60	8458
50		0.00	82.95	0.01	9.79	16.63	0.00	4.51	0.28	0.17	21.48	9959
111		16.41	37.46	0.01	16.81	7.84	0.01	3.89	0.64	0.07	16.32	2.76
160		29.64	20.17	0.01	18.11	4.68	0.01	3.73	0.62	0.02	16.30	0.84
210		25.46	9.27	0.01	12.80	2.42	0.01	2.84	0.49	0.00	11.74	0.46
260		23.63	5.31	0.02	12.36	1.62	0.03	1.71	0.41	0.00	10.06	0.29
310		29.01	5.00	0.01	12.05	1.89	0.12	2.35	0.37	0.00	11.70	0.24
360		25.63	8.44	0.02	9.97	3.06	0.14	3.20	0.32	0.00	11.47	0.45
410		28.11	9.97	0.02	10.64	7.36	0.13	4.56	0.29	0.08	13.57	0.62
460		10.50	18.91	0.01	9.62	10.30	0.09	5.56	0.29	0.22	10.67	2.78
505		0.00	0.82	0.02	4.21	1.21	0.00	13.47	0.00	0.00	2.18	203

the bottom of a soil pit in Huntingdon, PA provided bedrock samples for the Marcellus black shale (Mathur et al., 2012).

3.2. REE analysis

For this study, bulk solid samples including rock fragments were air-dried and ground to pass through a 100-mesh sieve (<150 μm). REE abundances were measured by SGS Canada Inc. (Minerals Services Laboratory at Toronto, Ontario; method IMS95A). In this analysis, 0.1g of ground sample was fused at 950 °C with lithium metaborate and re-dissolved in dilute nitric acid. Resultant solutions were analyzed by inductively coupled plasma mass spectrometer (ICP-MS) for rare earth elements and Zr (analytical details can be found at www.ca.sgs.com). For quality assessment and control, randomly-selected samples were run as duplicates and the precision was estimated at $\pm 5\%$. In addition, two USGS rock standards (BCR-2 and W-2) were analyzed as unknown samples and reported REE concentrations were compared to reference values. The relative errors observed were less than 10%, except for Tm ($\sim 15\%$).

3.3. Characterization of cation exchangeable capacity (CEC)

Cation concentrations in the exchangeable pools of the soils were characterized following the same procedure as Jin et al. (2010). Specifically, about 2.5 g of a sample were weighed into a 50-ml centrifuge tube and 25 ml of 0.1 M BaCl_2 -0.1 M NH_4Cl solution were added. Slurry was shaken vigorously on the shaker table for 15 min, and then centrifuged at 2500 rpm for 20 min. The solution was filtered, weighed and analyzed by inductively coupled plasma optical emission spectrometry for major elements at the Low-Temperature Geochemistry Laboratory of the University of Texas at El Paso. Standards were prepared in 0.1M BaCl_2 -0.1M NH_4Cl solution to ensure matrix matching.

4. Results

4.1. REE in shale parent materials

Parent materials for the two PA sites (gray shale and black shale) have been previously discussed in details (Jin et al., 2010; Ma et al., 2011; Mathur et al., 2012). A drill core (DC-1) at the Shale Hills catchment was assumed to allow characterization of the gray shale parent bedrock: total REE contents in DC-1 are 220–276 ppm (average concentration: 244 ppm, $\sim 40\%$ higher than the North American Shale Composite; Table 2). REE-rich phosphate minerals (e.g., $\sim 20 \mu\text{m}$ size particles) are commonly observed in the shale bedrock under scanning electron microscope (Ma et al., 2011). Rock chips (AF-1-17) from the bottom of a soil pit in Huntingdon, PA provided samples for the Marcellus black shale (Mathur et al.,

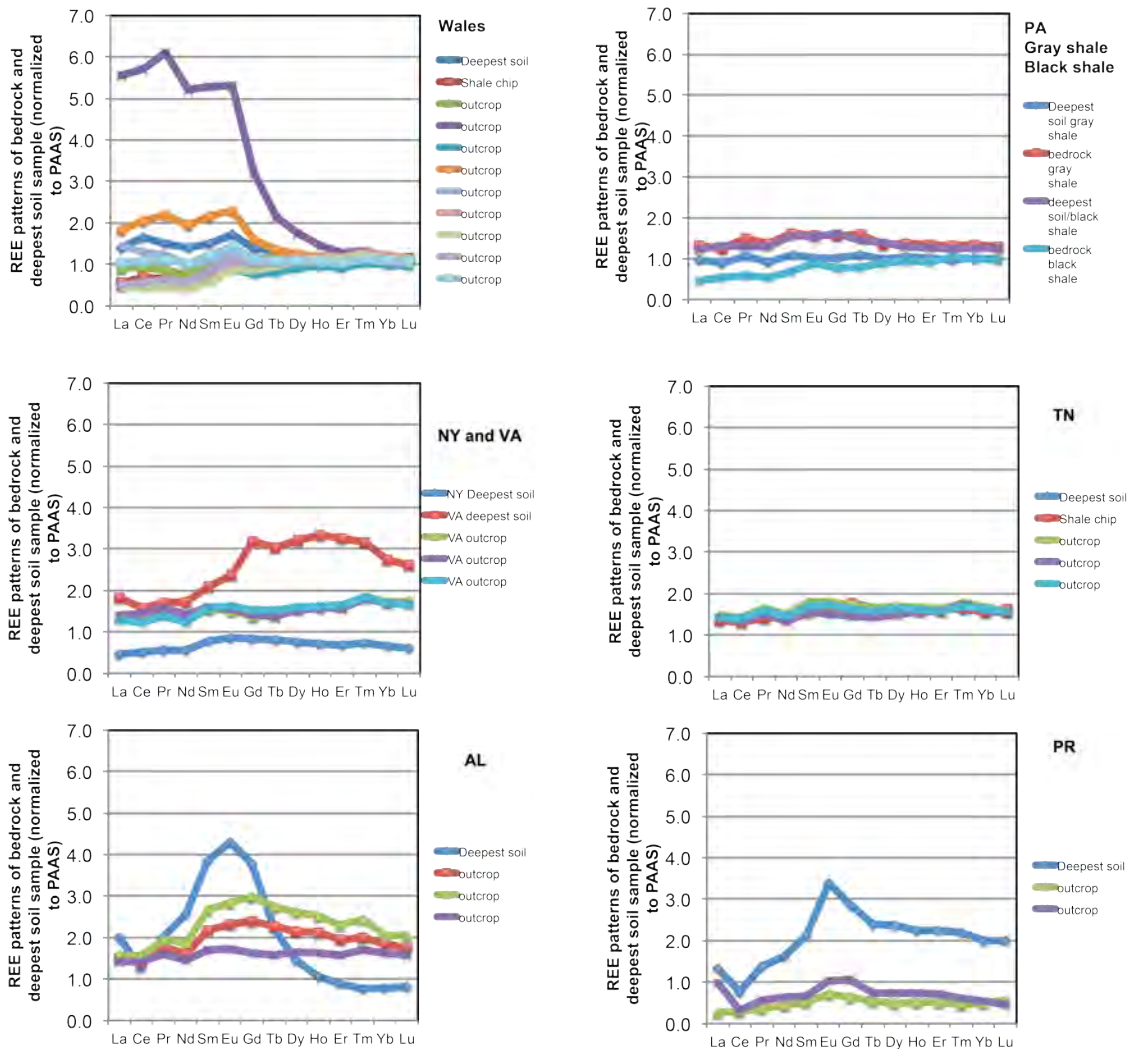


Fig. 2. REE patterns (normalized to PAAS composite) of deepest soil, rock chips, and local outcrop samples for all eight study sites.

2012; Jin et al., 2013): total REE content is ~468 ppm (Table 2), ~100% higher than that of the Rose Hill gray shale at PA.

Unlike the shale parent materials in the PA sites that have been characterized for their REE contents, parent materials for the other soil profiles have been only studied for major element compositions (Dere et al., 2013; Dere, 2014). At each site, we selected rock chips collected from bottom of soil pits and rock samples collected from nearby outcrops to analyze for REE contents. These bedrocks are from the same or equivalent units of Rose Hill shales and their major elemental chemistry varies little among sites except for Ca (Dere et al., 2013), but REE contents vary significantly (Table 2). Indeed, the total REEs measured in all rocks range from 63 to 356 ppm, with an outlier of 966 ppm. Among all seven sites, Wales and PR bedrocks have the most variable REE contents. In addition to bedrock from local outcrops and rock chips in soil pits, the deepest soils in soil pits can be practically used as parent materials to study elemental mobility.

Elemental concentrations of REE in rocks and deepest soils are normalized to Post-Archean Austrian Shale (PAAS), the well-known shale units (Figure 2). Overall, the patterns are flat, except for three outliers. One outcrop from Wales is really high in light REEs (LREE) while the deepest soils from AL and PR sites are more enriched in middle REEs (MREE). In this study, the deepest soil sample from the TN site show total REE content and REE distribution patterns similar to the rock fragments (Table 2 and Figure 2), consistent with the inference that in general the deepest soil samples should be chemically most similar to the parent material. However, the assumed parent materials from the Wales, AL, and PR sites are significantly different from the deepest soils in respective soil profiles in that 1) total REE contents in these rock samples are too low compared to some soils to be considered as parent materials for REE and 2) general REE patterns are different from the above soil samples (Figure 2). Hence, we conclude that in this study, our selected rock samples from Wales, AL, and PR are not representative of the parent materials in term of REE contents. Our follow-up study is measuring REEs in other available rock samples from these sites (Dere et al., 2013) to better constrain the REE parent compositions. In the following discussion, we will use the deepest available soil samples from each site as the assumed parent materials for REE contents.

4.2. Total REE in eight soil profiles

Northern sites of the shale weathering transect (Wales, PA, NY, VA) have relatively thin soil profiles with soil thickness ranging from 30 to 80 cm, except for the NY site which is developed on glacial till (soil thickness = 230 cm) and for the PA black shale site (soil thickness = 170 cm) (Table 1). In contrast, southern sites (TN, AL, PR) have much thicker soils, up to 600 cm.

Total REE contents vary significantly with depth and also among eight soil profiles (Figure 3). Total REE contents in the Wales, PA and VA profiles range from ~ 170 to 340 ppm. REE contents in the PA black shale profile (124-243 ppm) show more variability as compared to the PA gray shale site (173-200 ppm); REE contents in the NY profile have a much narrower range from 102 to 169 ppm. REE contents generally decrease towards the surface, but for PR, AL, PA-black and VA sites, slight higher REE concentrations are observed at depth right above the depth of auger refusal (i.e., the deepest soil).

4.3. REE patterns in the soils

REE patterns of soil samples are normalized to those of their responding parents (the deepest soils, for the reasons discussed in Section 4.1) (Figure 4). Three northern sites (Wales, PA, and NY) and TN have relatively flat pattern, with concentration ratios of soils to parent close to 1. This indicates the degree of REE depletion is low and also REEs are lost proportionally (without fractionation) during soil genesis and rock weathering. In contrast, three southern sites (VA, AL, and PR) have significantly deviated from parent composition in both total concentrations and REE patterns. Indeed, for different depths in each weathering profile, soils are depleted in REEs at shallow depths while deeper soils are enriched, consistent with Figure 3. Moreover, for a given soil sample normalized to parent, the REE pattern is not flat. For example, most of soils in VA site experience more loss (proportionally) in heavy REE (HREE) than in LREE and MREE. For AL and PR sites, however, most soils are more depleted in the LREE. At each site, soils that are enriched in REE exhibit REE patterns that are complementary to those shown in soils of REE losses. For the PA-black shale (Marcellus shale) site, soils with lower REE contents are depleted in MREE, and soils that accumulate REE are more enriched in MREE. For soils at the PR site, Ce shows strong positive anomaly.

4.5. CEC of soil profiles

The CEC of soils vary among sites and also with depth (Table 4). CEC is overall higher at PR than at other sites; within PR site, CEC decreases sharply with depth. Soils from other sites have relative lower CEC, and the depth trends are also variable.

The soil pH values were measured and reported by Dere et al. (2013) and they ranged from 2.8 to 3.8 for all sites except for PR. PR soils were less acidic, with pH ranging from 4 to 5.5. The relative concentrations of cations that are adsorbed to the exchangeable sites are pH-dependent: higher proportions of divalent cations are observed in soils with higher pH but Al predominates in soils at lower pH (Appendix Figure 1). Dere et al. (2013) reported up to 20 wt.% of Ca in PR shales, much higher than those in other Rose Hill transect sites (< 1 wt%). This explains higher pH and CEC, as well as higher (Ca+Mg)/Al ratios in the exchangeable sites at PR.

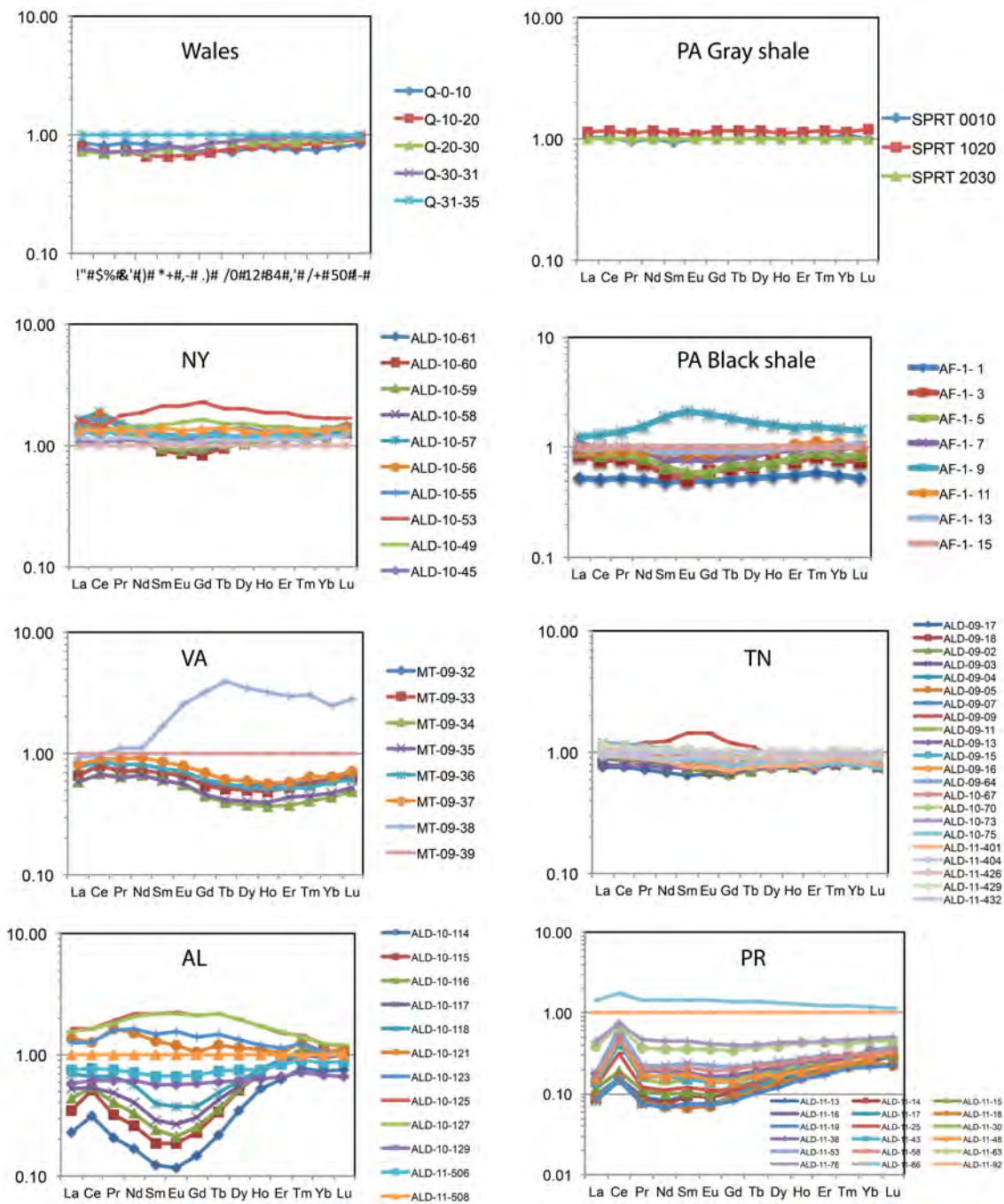


Fig. 4. REE patterns (normalized to deepest soil in each soil profile) of soils from all eight study sites.

5. Discussion

5.1. REE mobility during shale weathering

One method for determining the extent of REE mobility is to measure the REE concentration change from an observed soil profile relative to the original concentrations in unweathered rock (April et al., 1986; Brimhall and Dietrich, 1987; Brimhall et al., 1992; White et al., 1998; Brantley et al., 2008; Brantley and White, 2009; Brantley and Lebedeva, 2011). Using this approach, relative changes in the concentration of the REE are compared to the concentration of an immobile element not involved in weathering. This approach has been used to estimate weathering extents of the dominant crystalline rocks (granite and basalt) as well as shale (e.g. April et al., 1986; White et al., 2001; Chadwick et al., 2003; Jin et al., 2010). The method is contingent upon the proper identification of the parent material.

The mass transfer coefficient, τ , is calculated to assess the mobility of REEs. The τ values can correct changes in elemental concentrations due to the effects of expansion/compaction and due to changes in other elements in the soils (Brimhall and Dietrich, 1987; Anderson et al., 2002):

$$\tau_{i,j} = \frac{C_{j,w}C_{i,p}}{C_{j,p}C_{i,w}} - 1 \quad (\text{Eq. 1})$$

Positive $\tau_{i,j}$ values indicate enrichment of element j, negative values mean depletion and zero means element j is immobile in the weathered soils (w) with respect to parent (p). Moreover, if $\tau_{i,j}$ is negative, it equals the fraction of element j that was lost from the soil and the relative enrichment factor for element j if $\tau_{i,j}$ is negative. The local outcrop bedrock samples, assumed parent materials as discussed above, are quite heterogeneous for each site, especially Wales. This suggests the trace metals in shales are quite variable and probably sensitive to local environments. Thus, we used the deepest soil sample from each profile for the $\tau_{i,j}$ calculation (p). Zr is used as immobile element i. The $\tau_{i,j}$ values computed for all profiles are reported in Table 5 and plotted in Figure 5.

The total REE and $\tau_{i,j}$ REE values at the NY site vary with depth and show a pattern that is distinct from the rest of sites, probably due to the nature of the region. NY site is on a glacial till so soils from this site might be developed on sediments of mixed bedrocks at all depths while at other sites soil development starts with the bedrock from depth. The NY site is not included in the comparison along the climatic gradient due to its unique nature of parent material.

A lower degree of REE depletion, up to 30%, is observed in soils of northern sites (Wales, PA-gray shale, PA-black shale). Between two sites in PA, black shales are more depleted than the gray shales (Figure 5). More extensive losses are observed in the southern sites. About 40% of REE are leached from

Table 5. Mass of RE depletion ($m_{j,w}$) and REE release rates in studied sites

Site	Sample	Depth cm	Total REE ppm	Zr ppm	Tau REE	Bulk density g/cm ³	Strain	Mj μg/cm ²	Rate ng/cm ² /yr			
Wales	Q-0-10	10	229	159	-0.14	0.88	0.52	-2528	-253			
	Q-10-20	20	202	169	-0.29	1.10	0.14					
	Q-20-30	30	200	176	-0.32	1.24	-0.02					
	Q-30-31	31	207	175	-0.29	1.25	-0.02					
	Q-31-35	35	279	166	0.00	1.28	0.00					
PA (gray shale)	SPRT 0010	5	175	273	-0.09	0.99	0.21	-98	-6			
	SPRT 1020	15	200	275	0.03	1.21	-0.02					
	SPRT 2030	25	173	246	0.00	1.33	0.00					
PA (Black shale)	AF-1- 1	2	124	85	-0.12	0.89	2.19	-1042	-61			
	AF-1- 3	41.5	184	132	-0.16	1.44	0.27					
	AF-1- 5	58	201	149	-0.19	1.51	0.07					
	AF-1- 7	73.5	235	170	-0.17	1.55	-0.08					
	AF-1- 9	104	342	154	0.33	1.60	-0.02					
	AF-1- 11	132.5	226	141	-0.04	1.63	0.05					
	AF-1- 13	150.5	236	150	-0.05	1.64	-0.02					
	AF-1- 15	170.5	243	146	0.00	1.65	0.00					
VA	MT-09-32	10	242	976	-0.35	1.05	0.33	-4925	-105			
	MT-09-33	20	239	977	-0.36	1.23	0.13					
	MT-09-34	30	205	742	-0.28	1.33	0.38					
	MT-09-35	40	206	672	-0.20	1.40	0.44					
	MT-09-36	50	263	800	-0.14	1.45	0.17					
	MT-09-37	60	284	871	-0.15	1.49	0.05					
	MT-09-38	70	470	1000	0.22	1.52	-0.10					
	MT-09-39	80	338	882	0.00	1.54	0.00					
TN	ALD-09-17	5	195	317	-0.39	1.12	0.28	8576	37			
	ALD-09-18	10	222	343	-0.35	1.20	0.11					
	ALD-09-02	20	221	305	-0.28	1.31	0.14					
	ALD-09-03	30	228	297	-0.23	1.39	0.10					
	ALD-09-04	40	247	289	-0.15	1.44	0.09					
	ALD-09-05	50	252	269	-0.06	1.48	0.14					
	ALD-09-07	70	273	263	0.04	1.54	0.13					
	ALD-09-09	90	304	253	0.20	1.57	0.15					
	ALD-09-11	110	268	273	-0.02	1.60	0.04					
	ALD-09-13	130	207	245	-0.16	1.62	0.15					
	ALD-09-15	150	265	222	0.19	1.63	0.26					
	ALD-09-16	155	262	213	0.23	1.63	0.31					
	ALD-09-64	170	297	212	0.40	1.64	0.31					
	ALD-10-67	200	269	216	0.24	1.66	0.27					
	ALD-10-70	220	285	213	0.34	1.66	0.29					
	ALD-10-73	240	243	167	0.46	1.67	0.63					
	ALD-10-75	250	247	151	0.63	1.67	0.80					
	ALD-11-401	270	234	209	0.12	1.68	0.30					
	ALD-11-404	300	245	280	-0.13	1.69	-0.03					
	ALD-11-426	340	275	289	-0.05	1.69	-0.07					
ALD-11-429	370	293	268	0.09	1.70	0.00						
ALD-11-432	398	268	268	0.00	1.70	0.00						
AL	ALD-10-114	10	79	258	-0.87	1.04	-0.13	-23785	-184			
	ALD-10-115	20	124	337	-0.84	1.14	-0.39					
	ALD-10-116	30	143	372	-0.83	1.22	-0.48					
	ALD-10-117	40	159	258	-0.73	1.28	-0.29					
	ALD-10-118	50	207	264	-0.66	1.33	-0.33					
	ALD-10-121	70	457	244	-0.18	1.40	-0.31					
	ALD-10-123	100	474	180	0.15	1.47	-0.11					
	ALD-10-125	120	628	173	0.59	1.50	-0.10					
	ALD-10-127	140	610	161	0.66	1.53	-0.05					
	ALD-10-129	155	203	119	-0.25	1.54	0.27					
	ALD-11-506	180	249	158	-0.31	1.57	-0.05					
	ALD-11-508	200	338	148	0.00	1.58	0.00					
	PR	ALD-11-13	8	28	135	-0.90	0.96			0.49	-129575	-512
		ALD-11-14	10	27	119	-0.89	0.99			0.64		
ALD-11-15		15	33	128	-0.87	1.06	0.42					
ALD-11-16		20	26	128	-0.90	1.12	0.35					

ALD-11-17	30	26	128	-0.90	1.21	0.25
ALD-11-18	40	26	131	-0.90	1.28	0.16
ALD-11-19	50	25	128	-0.91	1.33	0.14
ALD-11-25	111	43	130	-0.84	1.50	-0.01
ALD-11-30	160	54	117	-0.78	1.56	0.06
ALD-11-38	210	63	120	-0.75	1.60	0.01
ALD-11-43	260	54	115	-0.78	1.62	0.03
ALD-11-48	310	59	117	-0.76	1.64	0.01
ALD-11-53	360	77	114	-0.67	1.66	0.02
ALD-11-58	410	65	125	-0.75	1.67	-0.07
ALD-11-63	460	107	131	-0.61	1.67	-0.12
ALD-11-76	505	123	119	-0.50	1.68	-0.03
ALD-11-86	580	355	105	0.63	1.69	0.09
ALD-11-92	632	237	114	0.00	1.69	0.00

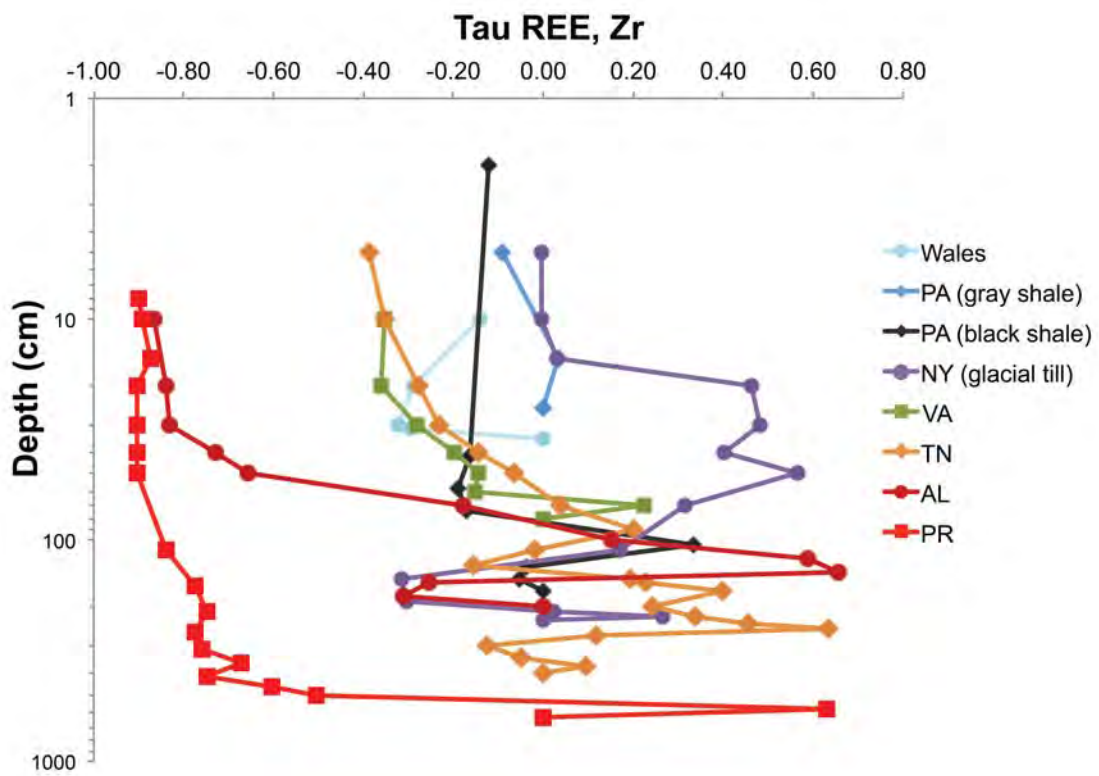


Fig. 5. Tau profiles for soils of the eight study sites.

top-soils at TN and VA. After that, soils slowly reach parent composition at about 80cm, but show variation at deeper depths. REE is almost 100% depleted from shallow soils at AL and PR. In general, the degrees of REE loss in shallow soils increase significantly from the northern sites to the southern sites, with climatic conditions in general becoming warmer and wetter along the climate transect.

The northern site soils (Wales and PA) show relative simple depletion patterns: the degree of REE depletion increase towards the surface. In the southern sites where soils are thicker (VA, AL and PR), REE shows depletion-addition profiles: REEs are leached from shallow soils but accumulate at deeper depths. The different behavior of REE in deeper soil profiles is further discussed in Section 5.3.

5.2. REE release rates along the climate transect

To quantitatively assess the loss of REE from each profile, the total mass of REE depletion at each site, $m_{j,w}$ is calculated using the following equation (Brimhall and Dietrich, 1987; Egli and Fitze, 2000; Herndon et al., 2011):

$$m_{j,w} = C_{j,p} \rho_p \int_0^L \frac{\tau(z)}{\varepsilon(z) + 1} dz \quad (\text{Eq. 2})$$

Here ρ_p and ρ_w are the bulk density of parent materials (p) and weathered soil. Negative $m_{j,w}$ values mean overall depletion of j from the entire soil profile while positive values mean net accumulation. The strain factor, $\varepsilon(z)$, is volume change factor, for depth z of the profile and can be calculated as:

$$\varepsilon(z) = \frac{C_{i,w} \rho_w}{C_{i,p} \rho_p} - 1 \quad (\text{Eq. 3})$$

Where positive ε values indicate soil expansion while negative ε values indicate soil compaction. However, if ε is 0, this suggests that soil genesis is an isovolumetric process.

Once the mass loss of an element has been calculated using Equation 2, an estimation of the duration of weathering allows determination of an elemental release rate, R_j (White, 2002; Brantley and White, 2009; Brantley and Lebedeva, 2011):

$$R_j = \frac{m_{j,w}}{SRT} \quad (\text{Eq. 4})$$

Similar exercise using above equations have been reported for major elements by Dere et al. (2013) and Dere (2014). $M_{j,w}$ and R_j data are presented in Table 5, and R_j are plotted against MAT and MAP in

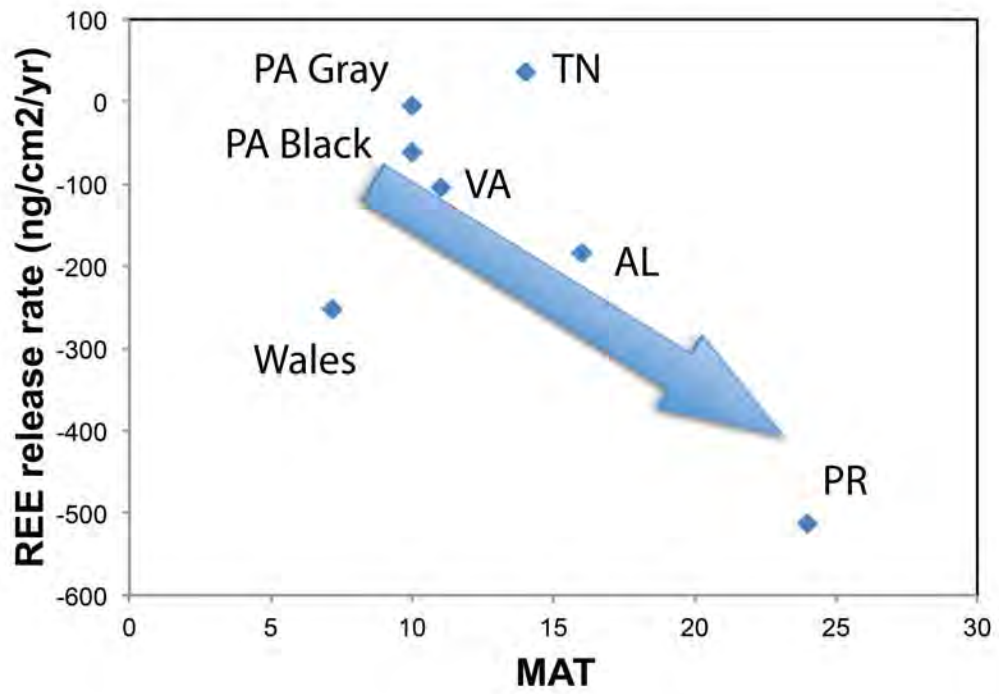
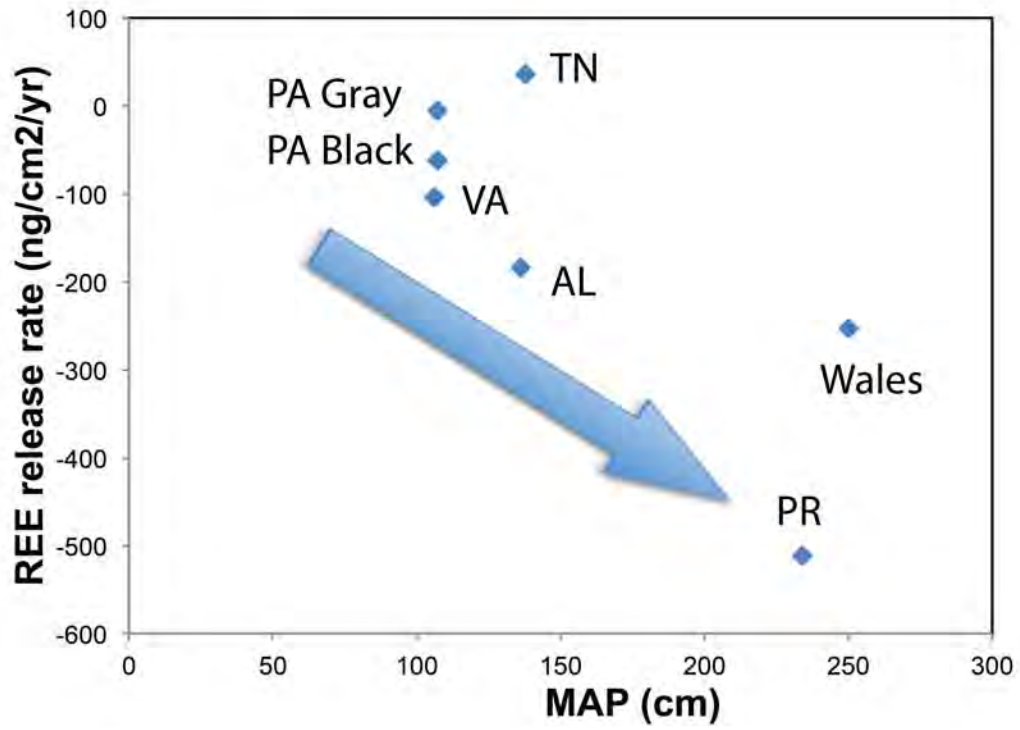


Fig. 6. REE release rates vs. MAT and MAP

Figure 6 for REEs. The loss rate of REE (R_j) ranges from 6 to 510 $\text{ng cm}^{-2} \text{yr}^{-1}$, with one exception where 37 $\text{ng cm}^{-2} \text{yr}^{-1}$ of REE are accumulated at TN.

Strong correlation is observed between R_j and MAT and between R_j and MAP (Fig. 6): higher precipitation and coupled higher air temperature enhance the leaching rates of REEs. Wales site is slightly off the trend, where lower MAT is compensated by high MAP. Similar correlations between mineral dissolution rates and environmental variables have been reported for major minerals or elements in rock types such as shales, basalts and granite (White and Blum, 1995; Williams et al., 2010; Rasmussen et al., 2011; Dere et al., 2013). MAP indicates availability of water, which can transport weathering products out of soils and promote future mineral dissolution. MAT dictates soil temperature, which is correlated to faster dissolution kinetics, especially for reactions with high activation energy. This study, for the first time, reported the dependence of REE release rates on climate conditions, and significant release of REE during shale weathering, especially under warm and humid conditions.

In addition, two PA sites have similar MAT and MAP, but black shale weathers fast and loses more REE than gray shales (Figure 6). This observation, in agreement with differences observed in major elements between two sites, suggests faster dissolution in OM-rich and sulfide-rich black shales. The net accumulation of REE at TN is unexpected. This could suggest either that dust inputs contribute an important flux of REEs or/and that parent materials at this location are heterogeneous and the deepest soil is not representative. The latter is unlikely given that TN parent samples that are collected from outcrops in close proximity and rock fragments from the soil pits have similar REE concentrations and patterns. Future study is needed to evaluate the sources of REE and quantify the flux of REE from dusts.

5.3. REE fractionation during shale weathering

Previous studies indicate aqueous REE signatures are inherited from rock REE signatures during weathering, but systematic fractionation of REEs commonly occurs during transport, and deposition (Nesbitt, 1979; Eldereld et al., 1990; Nesbitt and Markovics, 1997; Shiller, 1997; Land et al., 1999; Viers et al., 2000; Aubert et al., 2001; Hannigan and Sholkovitz, 2001; Compton et al., 2003; Bau et al., 2004; Johannesson et al., 2004; Andersson et al., 2006; Stille et al., 2006). Numerous environmental factors are known to control REE fractionation and redistribution including soil pH, complexation, adsorption and re-precipitation. For example, REEs are more soluble and MREEs are more enriched than LREEs and HREEs at acidic conditions. In addition, enhanced mobility of certain REEs can be due to preferred dissolution of REE-rich trace minerals. Indeed, phosphate minerals, such as rhabdophane, dissolve to preferentially release MREE from shales (Ma et al., 2011).

Soils at the northern sites have experienced low extent of weathering, as no significant loss is observed for major minerals and also for REEs (Dere et al., 2013; Figure 4). In the southern sites, more

REE is depleted from soils and REE is more systematically fractionated. For PR and AL sites, particularly, LREE and MREE are more depleted in shallow soils but enriched in deeper ones. When these samples were collected, a clayey layer was reached at the bottom of the pit to prevent from digging and augering further. Also, more clays and Fe-oxyhydroxide are present in these soil profiles (Dere et al., 2013; Dere, 2014). This study observed much higher CEC in PR site, indicative of higher clay contents. Thus we suggest that elemental fractionation within the REE group is induced when soluble REE is adsorbed to secondary Fe phases and clays.

Soils from the VA site, however, are more depleted in HREE at shallow depths and enriched in deeper depths. REEs form more stable solution complexes with increasing atomic numbers (Wood, 1990; Lee and Byrne, 1993; Luo and Byrne, 2004), making solutes HREE enriched and leaving the residue more LREE enriched. Thus it is reasonable to assume that REEs are mobilized by chelating with other ions including dissolved organic matter.

Ce has more than one oxidation state and this gives rise to redox-induced Ce anomalies and thus records changes of redox conditions in geological processes (e.g., Brookins, 1989; McLennan, 1989; Prudencio et al., 1995; Bau, 1999; Patino et al., 2003; Ma et al., 2011). Ce anomaly observed in PR and AL probably points to the fluctuation in reduction-oxidation conditions in these sites, due to high MAP and thick soil profiles. Dere et al. (2013) and Dere (2014) have reported redoximorphic features in these soils.

6. Summary

We systematically studied REE mobility and fractionation during shale weathering along a climate gradient. About 30 bedrock samples and 90 soil samples from eight study sites in eastern USA and Wales, UK were analyzed for REE and other trace element concentrations and selected soil and bedrock samples were characterized for cation exchange pools (such as Ca, Mg, K, Na, Al, Fe) in this study. Mass balance models were applied to quantify the release rates of REE from each site. The results show that both temperature and precipitation governs the dissolution rates of REE-bearing minerals, and thus the overall loss of REE. Significant release of REE is observed during shale weathering, especially under warm and humid conditions. In two PA sites of similar climate conditions, black shales tend to be more depleted of REE than gray shales. REE fractionation is more pronounced in southern sites where more REE is lost under warm and humid conditions, and general patterns suggest more complex depletion and accumulation of REE in soil profiles. This study improved our understanding of the geochemical behaviors of these critical elements during chemical weathering by studying solid weathering products and parent materials. Shale weathering on continents is an important component to understand global REE cycles at Earth's surface. Future studies are needed to characterize the transport

and deposition of REE from shale weathering, especially those on REE-bearing trace minerals on microscopic scales and on REE mobilization by natural waters.

The following abstracts and invited presentations have resulted from the work supported by this USGS grant and one manuscript is currently being prepared in submission to *Chemical Geology*.

- Ma, L., Jin, L., Dere, A., White, T., Mathur, R. Brantley, S. (2012) How lithology and climate affect REE mobility and fractionation along a shale weathering transect of the Susquehanna Shale Hills Critical Zone Observatory. AGU annual meeting (San Francisco, CA, 2012)
- Ma, L., Chabaux, F., Dere, A., White, T., Jin, L., Brantley S. (2012) Using U-series isotopes to quantify regolith formation rates and chemical weathering timescales along a shale transect within the Susquehanna Shale Hills Critical Zone Observatory. AGU annual meeting (San Francisco, CA, 2012)
- Jin, L., Ma, L., Dere, A., White, T., and Brantley, S. (2014) Systematic investigation of REE mobility and fractionation during continental shale weathering along a climate gradient. AGU annual meeting (San Francisco, CA, 2014)

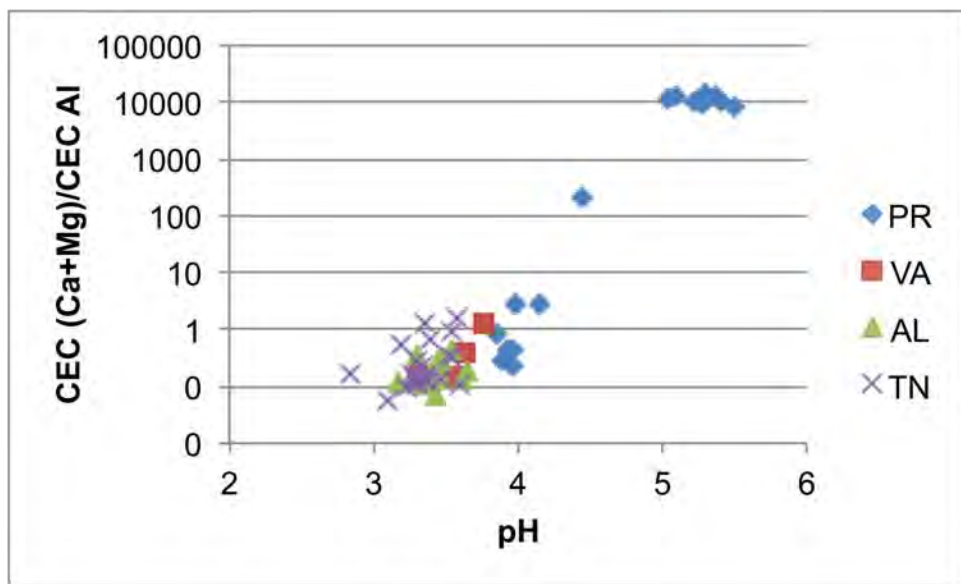


Fig A1. CEC (Ca+Mg)/CEC Al vs. soil pH

References

- Anderson, S. P., Dietrich, W. E. and Brimhall, G. H. (2002) Weathering profiles, mass-balance analysis, and rates of solute loss: Linkages between weathering and erosion in a small, steep catchment. *GSA Bulletin* **114**, 1143- 1158.
- Andersson, K., Dahlgqvist, R., Turner, D., Stolpe, B., Larsson, T., Ingri, J., and Andersson, P. (2006) Colloidal rare earth elements in a boreal river: changing sources and distributions during the spring flood. *Geochimica Cosmochimica Acta* **70**, 3261-3274.
- April, R. H., Hluchy, M. M. and Newton, R. M. (1986) Chemical weathering in two Adirondack watersheds: Past and present-day rates. *Geol. Soc. Am. Bull.* **97**:1232-1238.
- Aubert, D., Stille, P., and Probst, A. (2001) REE fractionation during granite weathering and removal by waters and suspended loads: Sr and Nd isotopic evidence. *Geochimica Cosmochimica Acta* **65**, 387-406.
- Bau, M. (1999) Scavenging of dissolved yttrium and rare earths by precipitating iron oxyhydroxide: experimental evidence for Ce oxidation, Y-Ho fractionation, and lanthanide tetrad effect. *Geochimica Cosmochimica Acta* **63**, 67-77.
- Bau, M., Alexander, B., Chesley, J.T., Dulski, P., and Brantley, S.L. (2004) Mineral dissolution in the Cape Cod aquifer, Massachusetts, USA: I. Reaction stoichiometry and impact of accessory feldspar and glauconite on strontium isotopes, solute concentrations, and REY distribution. *Geochimica Cosmochimica Acta* **68**, 1199-1216.
- Birkeland P. W. (1999) *Soils and Geomorphology*. Oxford University Press, New York. p. 430.
- Bockheim J. G. (1980) Solution and use of chronofunctions in studying soil development. *Geoderma* **24**, 71-85.
- Brantley, S. L. and Lebedeva, M. (2011) Learning to read the chemistry of the regolith to understand the critical zone. *Annu. Rev. Earth Pl. Sc.* **39**, 387-416.
- Brantley, S. L. and White, A. F. (2009) Approaches to modeling weathered regolith. *Rev. Mineral. Geochem.* **70**, 435-484.
- Brantley, S. L., Bandstra, J., Moore, J. and White, A. F. (2008) Modeling chemical depletion profiles in regolith. *Geoderma* **145**:494-504.
- Brantley, S. L., Goldhaber, M. B. and Ragnarsdottir, K. V. (2007) Crossing disciplines and scales to understand the critical zone. *Elements* **3**, 307–314.
- Brimhall, G. H. and Dietrich, W. E. (1987) Constitutive mass balance relations between chemical composition, volume, density, porosity, and strain in metasomatic hydrochemical systems: Results on weathering and pedogenesis. *Geochim. Cosmochim. Acta* **51**, 567-587.
- Brimhall, G. H., Chadwick, O. A., Lewis, C. J., Compston, W., Williams, I. S., Danti, K. J., Dietrich, W. E., Power, M. E., Hendricks, D. and Bratt, J. (1992) Deformational mass transport and invasive processes in soil evolution. *Science* **255**:695-702.
- Brookins, D.G. (1989), Aqueous geochemistry of rare earth elements. *Reviews in Mineralogy* **21**, 201-225.
- Cadwell, D. H. and Muller, E. H. (2004) New York glacial geology, U.S.A. In J. Ehlers and P. L. Gibbard (eds.) *Quaternary Glaciations – Extent and Chronology. Part II: North America*. Elsevier, Netherlands. pp. 201-205.
- Chadwick, O. A., Gavenda, R. T., Kelly, E. F., Ziegler, K., Olson, C. G., Elliott, W. C. and Hendrick, D. M. (2003) The impact of climate on the biogeochemical functioning of volcanic soils. *Chem. Geol.* **202**:195-223.
- Ciolkosz, E. J., Cronce, R. C. and Sevon, W. D. (1986) Periglacial features in Pennsylvania. *Pa. State Univ., Agron. Ser.* **92**. 52 p.
- Clark, G. M. and Ciolkosz, E. J. (1988) Periglacial geomorphology of the Appalachian highlands and interiorhighlands south of the glacial border – a review. *Geomorphology* **1**, 191-220. Clark C. D., P. L. Gibbard and Rose J. (2004) Pleistocene glacial limits in England,

- Scotland and Wales. In J. Ehlers and P. L. Gibbard (eds.) *Quaternary Glaciations – Extent and Chronology. Part I: Europe*. Elsevier, Netherlands. pp. 47-82.
- Compton, J.S., White, R.A., and Smith, M. (2003) Rare earth element behavior in soils and salt pan sediments of a semi-arid granitic terrain in the Western Cape, South Africa. *Chemical Geology* 201, 239-255.
- Dere, A.L., White, T.S., April, R.H., Reynolds, B., Miller, T.E., Knapp, E.P., McKay, L.D., Brantley, S.L. (2013) Climate dependence of feldspar weathering in shale soils along a latitudinal gradient, *Geochimica et Cosmochimica Acta* 122, 101-126, doi: <http://dx.doi.org/10.1016/j.gca.2013.08.001>
- Dere, A.L. (2014) *Shale Weathering across a latitudinal climosequence*. PhD thesis, the Pennsylvania State University, 302 pages.
- Egli, M. and Fitze, P. (2010) Formulation of pedogenic mass balance based on immobile elements: a revision. *Soil Sci.* 165, 437–443.
- Elderfield, H., Upstill-Goddard, R., and Sholkovitz, E.R. (1990), The rare earth elements in rivers, estuaries, and coastal seas and their significance to the composition of ocean waters. *Geochimica Cosmochimica Acta* 54, 971-991.
- Gardner, T. W., Ritter, J. B., Shuman, C. A., Bell, J. C. Sasowsky, K. C. and Pinter, N. (1991) A periglacial stratified slope deposit in the valley and ridge province of central Pennsylvania, USA: sedimentology, stratigraphy and geomorphic evolution. *Permafrost Periglac. Process.* 2:141-162.
- Hannigan, R.E., and Sholkovitz, E.R. (2001) The development of middle rare earth element enrichments in freshwaters: weathering of phosphate minerals. *Chemical Geology* 175, 495-508.
- Herndon, E.M., Jin, L., and Brantley, S.L. (2011) Soils reveal widespread Manganese enrichment from industrial inputs. *Environmental Sciences and Technology* 45(1), 241-247.
- Imbrie, J., Hays, J. D., Pisias, N. G., Prell, W. L. and Shackleton, N. J. (1984) The orbital theory of Pleistocene climate: support from a revised chronology of the marine $\delta^{18}O$ record. In J. I. A. Berger, J. Hays, G. Kukla and B. Saltzman (eds.) *Milankovitch and climate*. Reidel, Dordrecht, Netherlands.
- Jenny, H. (1941) *Factors of soil formation*. McGraw Hill, NY. 281 p.
- Jin, L., Ravella, R., Ketchum, B., Heaney, P. and Brantley, S. L. (2010) Mineral weathering and elemental transport during hillslope evolution at the Susquehanna/Shale Hills Critical Zone Observatory. *Geochim. Cosmochim. Acta.* 74, 3669-3691.
- Jin, L., Rother, G., Cole, D. R., Mildner, D. F. R., Duffy, C. J. and Brantley, S. L. (2011) Characterization of deep weathering and nanoporosity development in shale – A neutron study. *Amer. Min.* 96:198-512.
- Johannesson, K.H., Tang, J., Daniels, J.M., Bounds, W.J., and Burdige, D.J. (2004) Rare earth element concentrations and speciation in organic-rich blackwaters of the Great Dismal Swamp, Virginia, USA. *Chemical Geology* 209, 271-294.
- King, P. B. and Ferguson, H. W. (1960) *Geology of northeasternmost Tennessee*: U.S. Geol. Survey Prof. Paper 311. 136 p.
- Koto, Y., Fujinaga, K., Nakamura, K., Takaya, Y., Kitamura, K., Ohta, J., Toda, R., Nakashima, T., and Iwamori, H. (2011) Deep-sea mud in the Pacific Ocean as a potential resources for rare-earth elements. *Nature Geoscience* 4, 535-539.
- Land, M., Ohlander, B., Ingri, J., and Thunberg, J. (1999) Solid speciation and fractionation of rare earth elements in a spodosol profile from northern Sweden as revealed by sequential extraction. *Chemical Geology* 160, 121-138.
- Lee, J.H. and Byrne, R.H. (1993) Complexation of trivalent rare earth elements (Ce, Eu, Gd, Tb, Yb) by carbonate ions. *Geochimica Cosmochimica Acta* 57, 295-302.
- Luo, Y.R. and Rynne, R. H. (2004) Carbonate complexation of yttrium and the rare earth elements in natural waters. *Geochimica Cosmochimica Acta* 68, 691-699.

- Lev, S.M. and Filer, J.K. (2004) Assessing the impact of black shale processes on REE and the U-Pb isotope system in the southern Appalachian Basin. *Chemical Geology* 206, 393-406.
- Ma, L., Jin, L., and Brantely, S.L. (2011) How mineralogy and slope aspect affect REE release and fractionation during shale weathering in the Susquehanna/Shale Hills Critical Zone Observatory. *Chemical Geology* 290, 31-49.
- Mathur, R., Jin, L., Prush, V., Paul, J., Ebersole, C., Fornadel, A., Williams, J. Z. and Brantley, S. (2012) Cu isotopes and concentrations during weathering of black shale of the Marcellus Formation, Huntingdon County, Pennsylvania (USA). *Chem. Geol.* 304:175-184.
- McLennan, S.M. (1989) Rare earth elements in sedimentary rocks: influence of provenance and sedimentary processes. *Reviews in Mineralogy* 21, 169-200.
- Nesbitt, H.W. (1979) Mobility and fractionation of rare earth elements during weathering of a granodiorite. *Nature* 279, 206-210.
- Nesbitt, H.W., and Markovics, G. (1997) Weathering of granodioritic crust, long-term storage of elements in weathering profiles, and petrogenesis of siliciclastic sediments. *Geochimica Cosmochimica Acta* 61, 1653-1670.
- Patino, L.C., Velbel, M.A., Price, J.R., and Wade, J.A. (2003) Trace element mobility during spheroidal weathering of basalts and andesites in Hawaii and Guatemala. *Chemical Geology* 202, 343-363.
- Prudencio, M.I., Gouveia, M.A., Sequeira Braga, M.A. (1995) REE distribution in present-day and ancient surface environments of basaltic rocks (central Portugal). *Clay Minerals* 30, 239-248.
- Rasmussen, C., Brantley, S., Richter, D., Blum, A., Dixon, J. and White, A. F. (2011) Strong climate and tectonic control on plagioclase weathering in granitic terrain. *Earth Planet. Sci. Lett.* 301, 521–530.
- Shiller, A.M. (1997) Dissolved trace elements in the Mississippi river: seasonal, interannual, and decadal variability. *Geochimica Cosmochimica Acta* 61, 4321-4330.
- Soil Survey Staff (1993) *National Soil Survey Handbook*, Title 430-VI. U.S. Govt. Printing Office, Washington, D.C.
- Stille, P., Steinmann, M., Pierret, M.-C., Gauthier-Lafaye, F., Chabaux, F., Viville, D., Pourcelot, L., Matera, V., Aouad, G., and Aubert, D. (2006) The impact of vegetation on REE fractionation in stream waters of a small forested catchment (the Strengbach case). *Geochimica Cosmochimica Acta* 70, 3217-3230.
- US Department of the Interior and US Geological Survey. *Mineral Commodity Summaries 2011* (US Government Printing Office, 2011).
- Viers, J., Dupre, B., Braun, J.-J., Deberdt, S., Angeletti, B., Ngoupayou, J.N., and Michard, A. (2000) Major and trace element abundances, and strontium isotopes in the Nyong basin rivers (Cameroon): constraints on chemical weathering processes and elements transport mechanisms in humid tropical environments. *Chemical Geology* 169, 211-241.
- White, A. F. (2002) Determining mineral weathering rates based on solid and solute weathering gradients and velocities: application to biotite weathering in saprolites. *Chem. Geol.* 190, 69–89.
- White, A. F. and Blum, A. E. (1995) Effects of climate on chemical weathering in watersheds. *Geochim. Cosmochim. Acta* 59, 1729– 1747.
- White, A. F., Blum, A. E., Schulz, M. S., Vivit, D. V., Stonestrom, D. A., Larsen, M., Murphy, S. F. and Eberl, D. (1998) Chemical weathering in a tropical watershed, Luquillo Mountains, Puerto Rico: I. Long-term versus short-term weathering fluxes. *Geochim. Cosmochim Acta* 62:209-226.
- White, A. F., Bullen, T. D., Schulz, M. S., Blum, A. E., Huntington, T. G. and Peters, N. E. (2001) Differential rates of feldspar weathering in granitic regolith. *Geochim. Cosmochim. Acta* 65, 847-869.

- Williams, J. Z., Bandstra, J. Z., Pollard, D. and Brantley, S. L. (2010) The temperature dependence of feldspar dissolution determined using a coupled weathering-climate model for Holocene-aged loess soils. *Geoderma* 156, 11-19.
- Wood, S.A. (1990) The aqueous geochemistry of the rare-earth elements and yttrium: 1. review of available low-temperature data for inorganic complexes and the inorganic REE speciation of natural waters. *Chemical Geology* 82, 159-186.